JACS
JOURNAL OF THE AMERICAN CHEMICAL SOCIETY
pubs.acs.org/JACS
Article

Mechanochemistry of Cationic Cobaltocenium Mechanophore

Yujin Cha, Tianyu Zhu, Ye Sha, Huina Lin, JiHyeon Hwang, Matthew Seraydarian, Stephen L. Craig, and Chuanbing Tang*

Cite This: J. Am. Chem. Soc. 2021, 143, 11871−11878
Read Online
ACCESS | Metrics & More | Article Recommendations | Supporting Information

ABSTRACT: Recent research on the mechanochemistry of metallocene mechanophores has shed light on the force-responsiveness of these thermally and chemically stable organometallic compounds. In this work, we report a combination of experimental and computational studies on the mechanochemistry of main-chain cobaltocenium-containing polymers. Ester derivatives of the cationic cobaltocenium, though isoelectronic to neutral ferrocene, are unstable in the nonmechanical control experimental conditions that were accommodated by their ferrocene analogs. Replacing the electron withdrawing C-ester linkages with electron-donating C-alkyls conferred the necessary stability and enabled the mechanochemistry of the cobaltocenium to be assessed. Despite their high bond dissociation energy, cobaltocenium mechanophores are found to be selective sites of main chain scission under sonomechanical activation. Computational CoGEF calculations suggest that the presence of a counterion to cobaltocenium plays a vital role by promoting a peeling mechanism of dissociation in conjunction with the initial slipping.

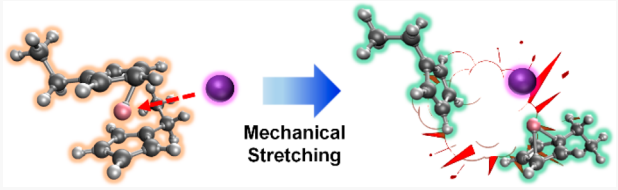

1. INTRODUCTION

Mechanophores, mechanically labile building blocks, continue to emerge as critical components in mechano-responsive polymers. Mechanical degradation of polymers causes the reduction in molecular weight, viscosity, and mechanical strength. The emergence of novel mechanophores has enabled new opportunities to open up mechanochemistry.[1−5] Several types of mechanophores have been investigated, including those that change color,[6−9] activate latent catalysts,[10,11] release small molecules,[12,13] empower self-strengthening materials,[14−17] and prepare conjugated polymers.[18]

Perhaps the classic mechanochemical response, however, remains as chain scission. Often, sites of preferential scission involve functional groups that have a low bond dissociation energy (BDE), such as peroxide,[19] diazo,[20] disulfide,[21] and thioether,[22] or even carbon−carbon bonds whose homolytic scission leads to the formation of persistent radicals.[23] It is now appreciated that mechanochemical bond scission can be quite mechanistically complex,[14,24,25] and that simple bond dissociation energy is an imperfect correlate of mechanical lability.[26] Recently, the mechanochemistry of metallocene-containing polymers has been explored.[27−30] Neutral metallocenes (e.g., ferrocene and ruthenocene) have been shown to act as highly selective sites of mechanical scission, despite the thermodynamically and chemically inert character associated with the high BDE of the metal-cyclopentadienyl (Cp) bond.

Cobaltocenium, which is isoelectronic to neutral ferrocene, represents a type of charged metallocene (or metallocenium) with high thermal and chemical stability.[31−33] The metal−ligand BDE of Co-Cp is reported to be significantly higher than that of ferrocene (102−195 kcal/mol vs 73−91 kcal/mol),[34−38] while the charged nature and the pairing of counterion also provide cobaltocenium with properties that have been used for applications of functional polyelectrolytes, including biomedicine and membranes.[39−47] The potential of cationic metallocenium mechanophores increases the likely significance of mechanistic considerations relative to their uncharged analogues: (1) potential contributions from the counterion to the mechanism of chain scission at the metal−ligand bond; (2) the anticipated greater influence of Cp substituents on metallocenium stability, especially electron-donating versus electron-withdrawing groups. The rich mechanochemistry of neutral metallocenes motivated us to explore cobaltocenium as a mechanophore.

Herein we report the design, synthesis, and mechanochemistry of main-chain cobaltocenium-containing polymers. The cobaltocenium is integrated into a polyoctene-like backbone with the aid of metathesis chemistry. Sonication was employed to carry out the mechanochemistry coupled with mechanistic trapping of scission intermediates. The results indicate that cobaltocenium possesses some unique mechano-responsive behaviors, different from the shearing mechanism of neutral metallocenes. Strikingly, computational models suggest that mechanical distortion of the complex facilitates access of the

Received: May 20, 2021
Published: July 20, 2021

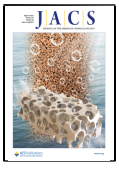

https://doi.org/10.1021/jacs.1c05233
J. Am. Chem. Soc. 2021, 143, 11871−11878

counterion to the exposed cobalt center, which in turns shifts the extent of the mechanical coupling.

2. RESULTS

2.1. Design Principle of Cobaltocenium Mechanophore. Assessing the mechanochemical reactivity of mechanophores requires that they be chemically stable under the conditions where mechanochemistry is performed. Typically, "non-mechanical" control experiments verify the necessary stability, but of course this needs not always be the case. Here, cobaltocenium derivatives and polymers were initially prepared following prior studies of the mechanochemistry of neutral ferrocene and ruthenocene (Figure 1).[27,28] A cobaltocenium

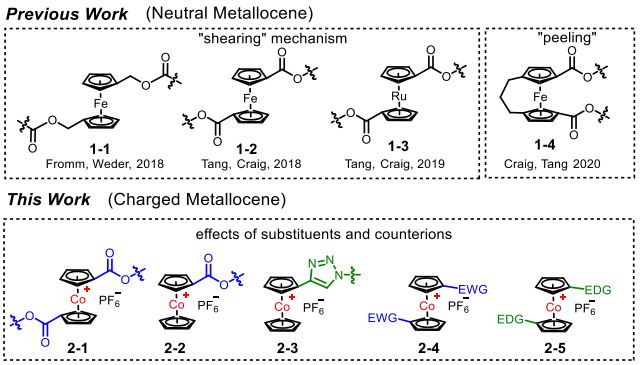

Figure 1. Structural design of metallocenes as mechanophores: comparison between neutral metallocenes (ferrocene and ruthenocene) and cationic cobaltocenium.

ester-linked dithioester was prepared as a chain transfer agent (CTA) and employed in the reversible addition-fragmentation chain-transfer (RAFT) polymerization of methyl methacrylate, affording cobaltocenium ester end-labeled poly(methyl methacrylate) (PMMA) (M_n= 77 000 Da, $Đ$ = 1.02) (Table 1, **P1**, Scheme S1). The use of end-functionalized polymer serves as a control for mechanical activation under pulsed ultrasonication of polymer solutions, as mechanical forces are focused on the center of the polymer chain. The solution of cobaltocenium end-labeled PMMA in dichloromethane (DCM) at a concentration of 2.5 mg/mL was exposed to an acoustic field with a power of 8.7 W/cm^2 and 50% duty cycle (1 s on and 1 s off) in an ice bath for 2 h and then characterized by ^{1}H and ^{19}F NMR. To our surprise, in contrast to the ruthenocene and ferrocene analogs, the cobaltocenium end group is not stable under these sonication conditions (Figure S1). The chemical instability remains when the dithioester CTA is replaced by a tertiary nitrile (Figure S2).

We hypothesized that the lack of stability might result from the presence of the ester linkage. Electron-withdrawing groups (EWG) (Figure 1, **2−1** and **2−2**) destabilize cobaltocenium due to the combination of reduced electron density on the Cp rings and the positively charged metal center.[45,46] We therefore replaced the C-ester linkage with a triazole, which serves as a weak electron-donating group (EDG) to the cobaltocenium Cp ligands (Figure 1, **2−3**). It was achieved by a click reaction between ethynyl cobaltocenium and the azide-modified chain transfer agent (Scheme S2).[48] As desired, this low molecular weight, electron-rich derivative showed no evidence of structural change by ^{1}H NMR in the sonication controls (Figure S3). The stability holds in an end-functionalized polymer control. Cobaltocenium triazole-linked PMMA was prepared by RAFT polymerization (M_n = 53,000 g/mol, $Đ$ = 1.03; see Table 1, **P2**, Scheme S2). As with the small molecular control, no evidence of change in either the cobaltocenium or PF_6^- counterion is observed under sonication (Figure S4).

Direct comparisons of small molecules and polymers containing cobaltocenium substituted with EDGs suggest that the EWGs contribute the decomposition of cobaltocenium. Though the less stable cobaltocenium under the sonication conditions does not rule out its possible mechanical susceptibility, it must be avoided in the structures to unambiguously explore the sole effect of mechanical stress. This finding suggests a useful consideration for the future design of cationic metallocenium as mechanophores.

2.2. Synthesis of Main-Chain Cobaltocenium-Containing Polymers. Following the initial investigations, a class of main-chain cobaltocenium-containing polymers was conceptualized using a simple polyoctene-like chain as the framework. This design considers (1) alkyl group as an EDG and (2) the exclusion of functional groups to eliminate

Table 1. Cobaltocenium-Containing Polymers Used in This Study

Polymer	Structure	M_n (Da)	$Đ$	Labeling molar ratio
P1	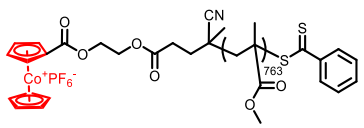	77,000	1.02	0.13%
P2	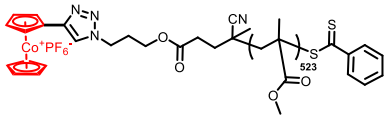	53,000	1.03	0.19%
P3	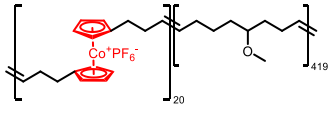	67,000	1.15	4.5%

https://doi.org/10.1021/jacs.1c05233
J. Am. Chem. Soc. 2021, 143, 11871−11878

unnecessary complications. A combination of ring-closing metathesis (RCM) and ring-opening metathesis polymerization (ROMP) was executed toward the synthesis of multiple cobaltocenium-labeled polymers. Multimechanophore labeling is more sensitive than a single mechanophore in mechanochemistry.[49] First, a diene compound **1** was prepared from lithium 1-butene-4-cyclopentadienide and $CoBr_2$ (Scheme 1 and the Supporting Information). Cyclic cobaltocenium monomer **2** was prepared by RCM of **1**. Cobaltocenium-containing polymer **P3** (M_n = 67,000 g/mol, $Đ$ = 1.15) was synthesized by copolymerization of **2** and 5-methoxycyclooctene in a similar approach to previous reports.[27,28]

Scheme 1. Synthesis of Cationic Cobaltocenophane and Main-Chain Cobaltocenium-Containing Copolymers

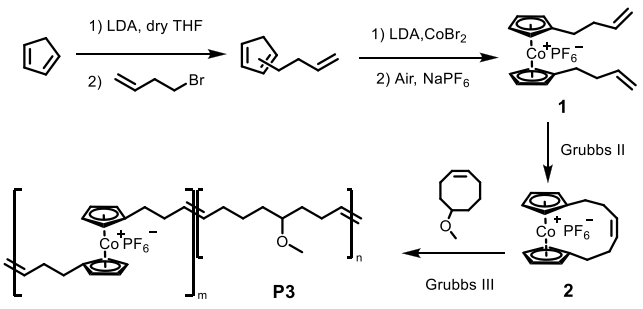

2.3. Mechanochemistry of Cobaltocenium Polymers. 1,1′-Dibutenyl cobaltocenium **1** was stable under prolonged sonication, further confirming the effect of EDGs (Figure S5). Sonication of **P3** was then conducted in DCM at a concentration of 2.5 mg/mL. Two-hour sonication led to a decrease in molecular weight from 67,000 g/mol to 46,000 g/mol (Figure 2C). The susceptibility of cobaltocenium was further characterized by the change in ^{1}H NMR. The Cp peaks from cobaltocenium significantly reduced with the emergence of new peaks corresponding to the formation of terminal cyclopentadiene after the sonication (Figure 2B and Figure S7). In addition, ^{19}F NMR also showed the decrease of PF_6^-, indicating the destruction of cobaltocenium (Figure S6). These results demonstrated that cobaltocenium is the preferential site of scission in the polymer chain.

We anticipated that the scission of cobaltocenium would resemble the heterolytic dissociation we observed previously in ferrocene and ruthenocene,[27,28] through which Co would maintain its +3 oxidation state in the free cation or its half-sandwich (Figure 2A). Following the earlier work on ferrocene, we employed 1,10-phenanthroline as a trap of the dissociated metal ions. **P3** was dissolved to a final concentration of 2.5 mg/mL in a 3.0 mM solution of 1,10-phenanthroline in DCM.

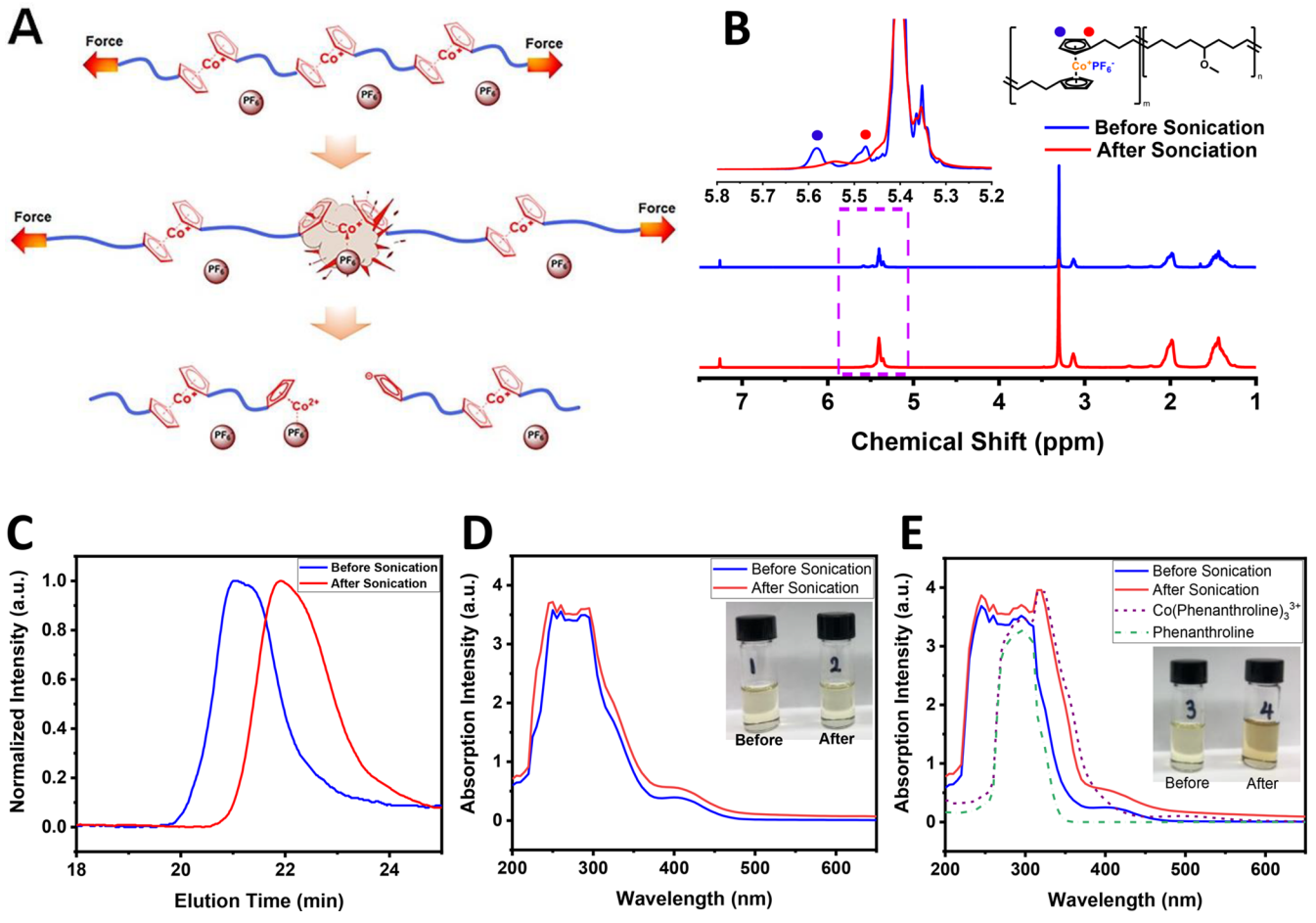

Figure 2. (A) Schematic illustration of cobaltocenium dissociation under ultrasonication for 2 h with a concentration of 2.5 mg/mL; (B) ^{1}H NMR spectra of **P3** before and after sonication; (C) GPC traces of **P3** before and after sonication; (D) UV−vis absorption spectra of **P3** without 1,10-phenanthroline before and after sonication; (E) UV−vis absorption spectra of 1,10-phenanthroline, $[Co(phenanthroline)_3]^{3+}$, and **P3** with 1,10-phenanthroline before and after sonication.

https://doi.org/10.1021/jacs.1c05233
J. Am. Chem. Soc. 2021, 143, 11871−11878

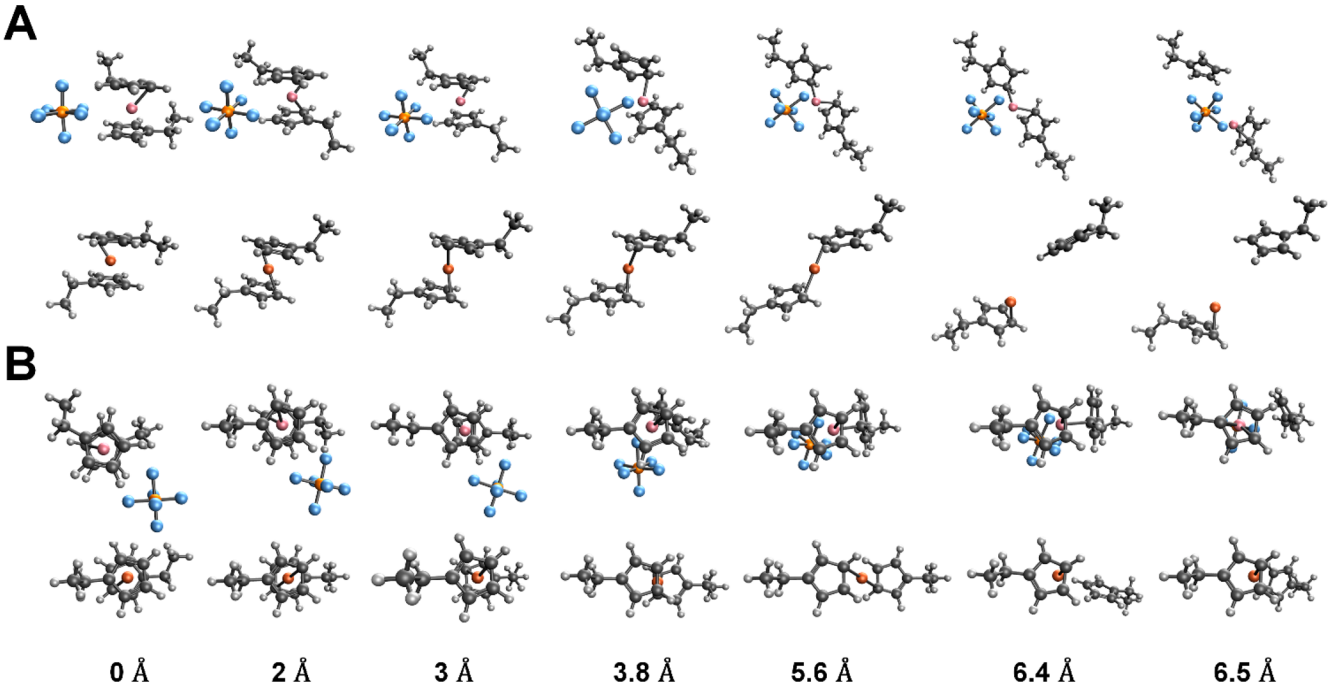

Figure 3. (A) Side view and (B) top view for the structural evolution of cobaltocenium (top panel) and ferrocene (bottom panel) model compounds with different stretching distances.

The solution was then subject to the same sonication conditions described above. The UV−vis absorption was compared before and after sonication. The results revealed the appearance of an absorption peak at 325 nm (Figure 2E, solid red line), which is assigned to the ligand to metal charge transfer of $[Co(phenanthroline)_3]^{3+}$. By contrast, sonication without 1,10-phenanthroline did not show any new absorption peaks (Figure 2D). In order to further confirm the assignment, we independently prepared $[Co(phenanthroline)_3]^{3+}$ and compared its UV−vis absorption spectrum to the sonication product.[50] As shown in Figure 2E (purple dashed line), the peak at 325 nm is similar to that of the product of polymer sonication. This result supports that the dissociation of cobaltocenium is heterolytic.

The presence of a counterion differentiates cobaltocenium from neutral metallocenes. To further understand the stretching and scission of cobaltocenium mechanophore, DFT calculations on 1,1′-diethyl cobaltocenium hexafluorophosphate were carried out using the constrained geometry simulating external force (CoGEF) method, which is often employed, with important caveats, to model mechanochemistry.[51,52] To mimic the elongation of the polymer backbone, the end-to-end distance between the carbon atoms of the two CH_3 groups of this model mechanophore was varied (Figure S8). As shown in Figure 3B, the Cp rings are aligned in a slightly staggered geometry at the fully relaxed state (the stretching distance is considered as 0). As the cobaltocenium is stretched by 2 Å, the two Cp rings rotate to orient two ethyl groups in the antiposition. With a further increase in end-to-end distance, the initially aligned two Cp rings start to slip so that the Co metal atom is no longer normal to the Cp centroids, resulting in a sharper increase of the system energy. This slipping of the parallel Cp ligands well resembles that of ferrocene.[27] However, further displacement results in dramatically different structural evolutions from what has been observed in ferrocene. As shown in Figure 3A, the simulated stretching of cobaltocenium leads to an onset of peeling motion in the Cp rings at approximately 3.8 Å. In comparison, ferrocene is still under the slipping process. Further stretching of this structure results in the elongation of the Co-Cp bond and further opens the peeled structure with an increased potential. The full dissociation of Cp takes place when the stretching distance reaches 6.5 Å, producing Cp^- and $[CpCo]^{2+}PF_6^-$. This dissociation mechanism is strikingly different from that of ferrocene. As shown in Figures 3A,B, ferrocene undergoes a chain slipping mechanism, but cobaltocenium has a mechanism of first slipping and then peeling.

One should acknowledge the limit of the CoGEF calculations, which characterize the chain scission behavior at essentially 0 K. In real cases, thermally assisted reactions would occur long before the force reaches the CoGEF calculated maximum. Even the specific thermally assisted pathway might differ from that calculated by CoGEF. Nevertheless, the calculations provide insights into the likely dissociation mechanism and reveal significant differences in cobaltocenium scission relative to its ferrocene analog. The energy increases until it reaches the first potential peak at 3.7−3.8 Å because of the distorted bond angle and bond distance with the onset of the peeling process (Figure 4A, blue symbol). When the stretching distance of cobaltocenium reaches 3.8 Å, the CoGEF potential abruptly decreases. A second decrease in potential energy occurs at 5.6 Å. Neither transition is observed in ferrocene dissociation, which proceeds through a smooth, single-step process (Figure S9). In addition, the maximum relative energy prior to dissociation (E_{max}) of cobaltocenium is lower than that of ferrocene. Furthermore, under the same pulling point and attachments of the model compounds, the maximum force (F_{max}) of cobaltocenium calculated over the stretching is significantly lower than that of ferrocene. F_{max} is 2.73 and 3.18 nN for cobaltocenium and ferrocene, respectively (Figure S10).

https://doi.org/10.1021/jacs.1c05233
J. Am. Chem. Soc. 2021, 143, 11871−11878

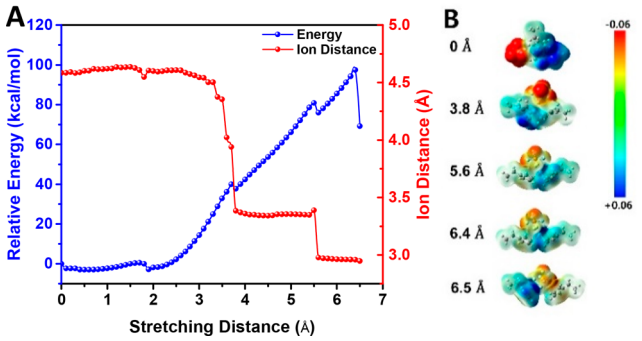

Figure 4. (A) CoGEF potential (system energy, blue symbol) and metal-ion (Co−P) distance (red symbol) as a function of the change in end-to-end distance and (B) representative electrostatic potential map of cobaltocenium as a function of the change in end-to-end distance (the contour surface is described based on van der Waals surface with an electron density of 0.001 e/Bohr^3 as proposed by Bader[53]).

We speculated that this difference in dissociation might be a result of the presence of a counterion. To examine the effect of the counterion during chain stretching, the distance of cobalt to PF_6^- was measured and compared to the CoGEF potential. As shown in Figure 4A (red symbol), the distance between cobalt(III) and phosphorus (Co−P) dramatically decreases at the energetic transition points (local maxima at 3.8 and 5.6 Å) noted above. We also calculated the distance of the metal center to the nearest fluoride (Co−F) (Figure S11), which shows a similar trend to that observed for Co−P. At these points, PF_6^- inserts between the two Cp rings (Figure 3B), facilitating the peeling of the sandwich structure. This observation can be explained by the coordinated interplay of stretching and Coulombic attraction. The stretching of cobaltocenium makes Cp rings slip, providing space for the PF_6^- anion to approach the cobalt cation, which is otherwise hindered by two Cp rings. This attraction guides the dissociation of cobaltocenium through a peeling-like pathway rather than slipping. Given that the calculated E_{max} and F_{max} for cobaltocenium are lower than those of ferrocene, it can be concluded that the counterion facilitates the bond dissociation, making cobaltocenium a more sensitive mechanophore.

To further examine the mechanism of bond cleavage, a molecular electrostatic potential (ESP) was used to depict the charge distribution during dissociation.[54] The representative ESP maps of the cobaltocenium model compound are shown as a function of stretching distance in Figure 4B. Before chain elongation, the charge distribution was biased on cobaltocenium and PF_6^-. At an added stretch of 3.8 Å, where the Cp is peeled off from the sandwich structure, the negative charge on PF_6^- starts to diminish. With the decreased distance between cobalt and PF_6^-, the charge separation is reduced through delocalization, stabilizing the system. After a single ligand dissociation is complete, the half-sandwich cobaltocenium holds a more positive charge, and the negative charge densities are distributed on PF_6^- and dissociated Cp^-. The ESP results support the heterolytic dissociation of cobaltocenium mechanophore, resulting in separated charge densities after dissociation.

We further explored how a change in counterion affects the calculated dissociation of cobaltocenium using a smaller Cl^- anion. The addition of Cl^- also contributes to a peeling-like dissociation mechanism, similar to PF_6^- (Figure S12). The interaction of cobalt(III) with Cl^- is stronger than with PF_6^-; Co(III) is considered to be a hard acid, which favors interactions with a harder base like Cl^- relative to the softer PF_6^-.[55] Consistent with the expectation of a stronger interaction, the use of Cl^- results in Cp dissociation at a shorter stretching distance (6.1 Å) and lower E_{max} (75.3 kcal/mol) than computed for PF_6^- (Figure S13).

3. DISCUSSION

Experimentally, both end group analysis and metal ion trapping indicate that the dissociation of cobaltocenium

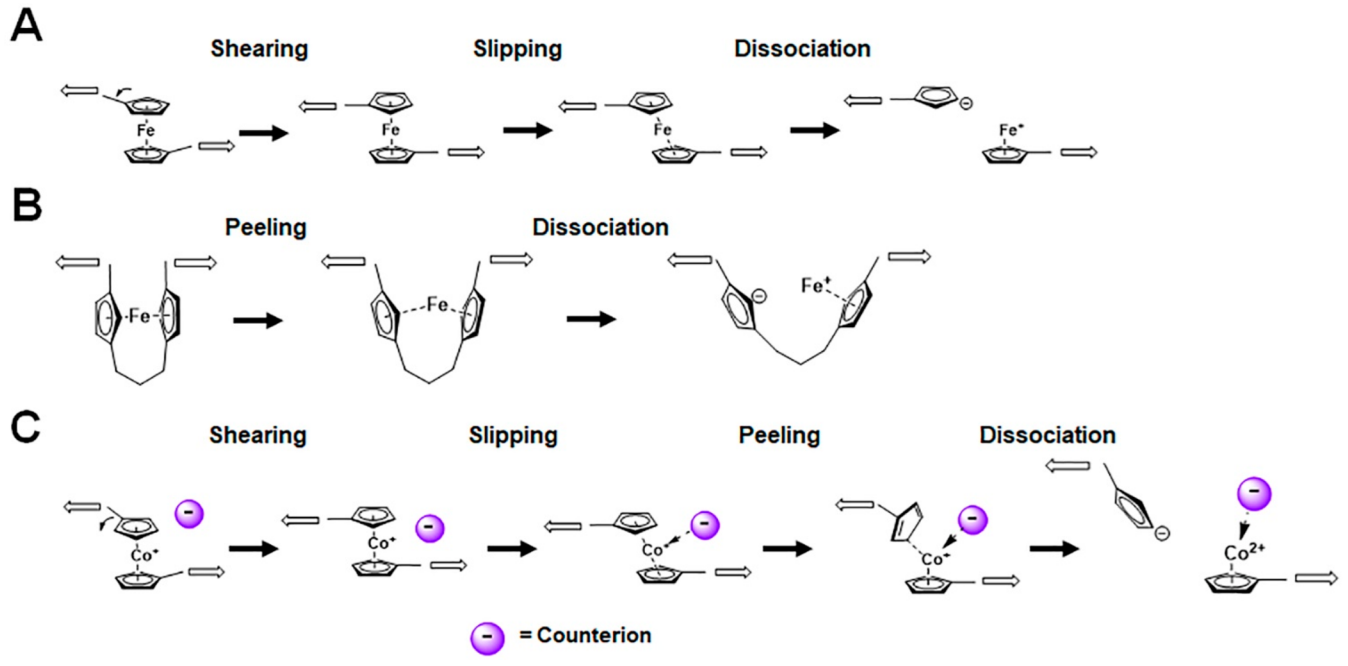

Figure 5. Proposed mechanisms of dissociation of mechanophores: (A) ferrocene, (B) *ansa*-ferrocenophane, and (C) cobaltocenium.

https://doi.org/10.1021/jacs.1c05233
J. Am. Chem. Soc. 2021, 143, 11871−11878

mechanophore is a net heterolytic process, in which the counterion in cobaltocenium might stabilize the dissociated cobalt ions even in the state of a partial half-sandwich structure. Though conceived differently, it was previously observed that the addition of external salts (tetrabutylammonium bromide) promotes the chain scission of ferrocene by stabilizing charge separation and/or anionic ligand exchange.[27]

The insights into dissociation mechanisms between cobaltocenium and ferrocene could be further gained by probing the change of coordination states of ligands to the metal center during stretching. We plotted the distances between Co and each carbon atom on one of the ligands versus the stretching distance. As shown in Figures S14 and S15, in the beginning of cobaltocenium, the coordination is η^5. However, once the Cp is peeled off at 3.8 Å, the coordination changes to η^1 based on the dramatic change of the Co−C distance. In the case of ferrocene, the coordination changes from η^5 to η^2 during the slipping process. We ascribe this difference in coordination to the increased coordination/charge donation provided by the associating counterion, which pushes the dissociating Cp to form the η^1 rather than η^2 state.

Different dissociative mechanisms, based on slipping and peeling, have been previously reported in metallocene mechanophores.[27,28] For instance, ferrocene and ruthenocene undergo slipping of Cp against an external force, leading to complete dissociation (Figure 5A). Very recently a peeling process was observed for ferrocenophane mechanophores in which Cp ligands are bridged by an alkyl tether.[30] The bridge serves as a conformational lock that restricts rotation along the Cp-Fe-Cp axle, inhibiting slipping and forcing the Cp to be peeled away from the nascent sandwich structure (Figure 5B). Here, an unbridged cobaltocenium mechanophore undergoes peeling-like dissociation not because of restricted conformations but due to the interaction between cobalt cation and counterion. The insertion of the counterion distorts the sandwich structure, resulting in a partial tilting of the Cp and contributions from peeling-type pathways (Figure 5C). Specifically, the partial shearing at the beginning opens the space to facilitate the interaction of the counterion with the metal center. This creates a CoGEF reaction path that differs from both ferrocene/ruthenocene and ferrocenophane.

4. CONCLUSIONS

In summary, we explored cationic cobaltocenium as a mechanophore and prepared main-chain cobaltocenium-containing copolymers via RCM and ROMP. It was discovered that cobaltocenium must be attached with EDGs, while EWGs would destabilize the mechanophore chemically, significantly different from ferrocene and ruthenocene. Although the cobaltocenium possesses high thermodynamic stability, it showed chain scission under an acoustic field. In contrast to neutral metallocenes in the absence of counterions, cobaltocenium has a different mechanism of chain scission, starting from the initial slipping followed by the peeling in the presence of the counterion, confirmed by the CoGEF computational studies. This new finding further expands the fascinating mechanochemistry of metallocenes.

■ ASSOCIATED CONTENT

Supporting Information

The Supporting Information is available free of charge at https://pubs.acs.org/doi/10.1021/jacs.1c05233.

Materials, characterization methods, sonication test, synthetic schemes, NMR spectra, and calculation details (PDF)

■ AUTHOR INFORMATION

Corresponding Author

Chuanbing Tang − *Department of Chemistry and Biochemistry, University of South Carolina, Columbia, South Carolina 29208, United States;* orcid.org/0000-0002-0242-8241; Email: tang4@mailbox.sc.edu

Authors

Yujin Cha − *Department of Chemistry and Biochemistry, University of South Carolina, Columbia, South Carolina 29208, United States*

Tianyu Zhu − *Department of Chemistry and Biochemistry, University of South Carolina, Columbia, South Carolina 29208, United States;* orcid.org/0000-0001-9115-6462

Ye Sha − *Department of Chemistry and Biochemistry, University of South Carolina, Columbia, South Carolina 29208, United States;* orcid.org/0000-0003-3338-1228

Huina Lin − *Department of Chemistry and Biochemistry, University of South Carolina, Columbia, South Carolina 29208, United States*

JiHyeon Hwang − *Department of Chemistry and Biochemistry, University of South Carolina, Columbia, South Carolina 29208, United States*

Matthew Seraydarian − *Department of Chemistry and Biochemistry, University of South Carolina, Columbia, South Carolina 29208, United States*

Stephen L. Craig − *Department of Chemistry, Duke University, Durham, North Carolina 27708, United States;* orcid.org/0000-0002-8810-0369

Complete contact information is available at: https://pubs.acs.org/10.1021/jacs.1c05233

Notes

The authors declare no competing financial interest.

■ ACKNOWLEDGMENTS

This work is supported by the National Science Foundation (NSF) under Grant CHE-1904016. The partial support from the NSF EPSCoR Program under Grant OIA-1655740 is acknowledged.

■ REFERENCES

(1) Deneke, N.; Rencheck, M. L.; Davis, C. S. An engineer's introduction to mechanophores. *Soft Matter* **2020**, *16* (27), 6230−6252.

(2) Izak-Nau, E.; Campagna, D.; Baumann, C.; Göstl, R. Polymer mechanochemistry-enabled pericyclic reactions. *Polym. Chem.* **2020**, *11* (13), 2274−2299.

(3) Ghanem, M. A.; Basu, A.; Behrou, R.; Boechler, N.; Boydston, A. J.; Craig, S. L.; Lin, Y.; Lynde, B. E.; Nelson, A.; Shen, H.; Storti, D. W. The role of polymer mechanochemistry in responsive materials and additive manufacturing. *Nat. Rev. Mater.* **2021**, *6* (1), 84−98.

(4) O'Neill, R. T.; Boulatov, R. The many flavours of mechanochemistry and its plausible conceptual underpinnings. *Nat. Rev. Chem.* **2021**, *5* (3), 148−167.

(5) Chen, Y.; Mellot, G.; van Luijk, D.; Creton, C.; Sijbesma, R. P. Mechanochemical tools for polymer materials. *Chem. Soc. Rev.* **2021**, *50* (6), 4100−4140.

(6) Sagara, Y.; Karman, M.; Verde-Sesto, E.; Matsuo, K.; Kim, Y.; Tamaoki, N.; Weder, C. Rotaxanes as Mechanochromic Fluorescent

Force Transducers in Polymers. *J. Am. Chem. Soc.* **2018**, *140* (5), 1584−1587.
(7) McFadden, M. E.; Robb, M. J. Force-Dependent Multicolor Mechanochromism from a Single Mechanophore. *J. Am. Chem. Soc.* **2019**, *141* (29), 11388−11392.
(8) Kosuge, T.; Zhu, X.; Lau, V. M.; Aoki, D.; Martinez, T. J.; Moore, J. S.; Otsuka, H. Multicolor Mechanochromism of a Polymer/Silica Composite with Dual Distinct Mechanophores. *J. Am. Chem. Soc.* **2019**, *141* (5), 1898−1902.
(9) Sagara, Y.; Traeger, H.; Li, J.; Okado, Y.; Schrettl, S.; Tamaoki, N.; Weder, C. Mechanically Responsive Luminescent Polymers Based on Supramolecular Cyclophane Mechanophores. *J. Am. Chem. Soc.* **2021**, *143* (14), 5519−5525.
(10) Wang, T.; Zhang, N.; Dai, J.; Li, Z.; Bai, W.; Bai, R. Novel Reversible Mechanochromic Elastomer with High Sensitivity: Bond Scission and Bending-Induced Multicolor Switching. *ACS Appl. Mater. Interfaces* **2017**, *9* (13), 11874−11881.
(11) Biewend, M.; Michael, P.; Binder, W. H. Detection of stress in polymers: mechanochemical activation of CuAAC click reactions in poly(urethane) networks. *Soft Matter* **2020**, *16* (5), 1137−1141.
(12) Lin, Y.; Kouznetsova, T. B.; Craig, S. L. A Latent Mechanoacid for Time-Stamped Mechanochromism and Chemical Signaling in Polymeric Materials. *J. Am. Chem. Soc.* **2020**, *142* (1), 99−103.
(13) Huo, S.; Zhao, P.; Shi, Z.; Zou, M.; Yang, X.; Warszawik, E.; Loznik, M.; Göstl, R.; Herrmann, A. Mechanochemical bond scission for the activation of drugs. *Nat. Chem.* **2021**, *13* (2), 131−139.
(14) Verstraeten, F.; Göstl, R.; Sijbesma, R. P. Stress-induced colouration and crosslinking of polymeric materials by mechanochemical formation of triphenylimidazolyl radicals. *Chem. Commun.* **2016**, *52* (55), 8608−8611.
(15) Gordon, M. B.; Wang, S.; Knappe, G. A.; Wagner, N. J.; Epps, T. H.; Kloxin, C. J. Force-induced cleavage of a labile bond for enhanced mechanochemical crosslinking. *Polym. Chem.* **2017**, *8* (42), 6485−6489.
(16) Pan, Y.; Zhang, H.; Xu, P.; Tian, Y.; Wang, C.; Xiang, S.; Boulatov, R.; Weng, W. A Mechanochemical Reaction Cascade for Controlling Load-Strengthening of a Mechanochromic Polymer. *Angew. Chem., Int. Ed.* **2020**, *59* (49), 21980−21985.
(17) Kida, J.; Aoki, D.; Otsuka, H. Self-Strengthening of Cross-Linked Elastomers via the Use of Dynamic Covalent Macrocyclic Mechanophores. *ACS Macro Lett.* **2021**, *10* (5), 558−563.
(18) Chen, Z.; Mercer, J. A. M.; Zhu, X.; Romaniuk, J. A. H.; Pfattner, R.; Cegelski, L.; Martinez, T. J.; Burns, N. Z.; Xia, Y. Mechanochemical unzipping of insulating polyladderene to semiconducting polyacetylene. *Science* **2017**, *357* (6350), 475−479.
(19) Encina, M. V.; Lissi, E.; Sarasúa, M.; Gargallo, L.; Radic, D. Ultrasonic degradation of polyvinylpyrrolidone: Effect of peroxide linkages. *J. Polym. Sci., Polym. Lett. Ed.* **1980**, *18* (12), 757−760.
(20) Berkowski, K. L.; Potisek, S. L.; Hickenboth, C. R.; Moore, J. S. Ultrasound-Induced Site-Specific Cleavage of Azo-Functionalized Poly(ethylene glycol). *Macromolecules* **2005**, *38* (22), 8975−8978.
(21) Larsen, M. B.; Boydston, A. J. Flex-Activated" Mechanophores: Using Polymer Mechanochemistry To Direct Bond Bending Activation. *J. Am. Chem. Soc.* **2013**, *135* (22), 8189−8192.
(22) Shiraki, T.; Diesendruck, C. E.; Moore, J. S. The mechanochemical production of phenyl cations through heterolytic bond scission. *Faraday Discuss.* **2014**, *170* (0), 385−394.
(23) Sumi, T.; Goseki, R.; Otsuka, H. Tetraarylsuccinonitriles as mechanochromophores to generate highly stable luminescent carbon-centered radicals. *Chem. Commun.* **2017**, *53* (87), 11885−11888.
(24) Nixon, R.; De Bo, G. Three concomitant C−C dissociation pathways during the mechanical activation of an N-heterocyclic carbene precursor. *Nat. Chem.* **2020**, *12* (9), 826−831.
(25) Chen, Z.; Zhu, X.; Yang, J.; Mercer, J. A. M.; Burns, N. Z.; Martinez, T. J.; Xia, Y. The cascade unzipping of ladderane reveals dynamic effects in mechanochemistry. *Nat. Chem.* **2020**, *12* (3), 302−309.
(26) Lee, B.; Niu, Z.; Wang, J.; Slebodnick, C.; Craig, S. L. Relative Mechanical Strengths of Weak Bonds in Sonochemical Polymer Mechanochemistry. *J. Am. Chem. Soc.* **2015**, *137* (33), 10826−10832.
(27) Sha, Y.; Zhang, Y.; Xu, E.; Wang, Z.; Zhu, T.; Craig, S. L.; Tang, C. Quantitative and Mechanistic Mechanochemistry in Ferrocene Dissociation. *ACS Macro Lett.* **2018**, *7* (10), 1174−1179.
(28) Sha, Y.; Zhang, Y.; Xu, E.; McAlister, C. W.; Zhu, T.; Craig, S. L.; Tang, C. Generalizing metallocene mechanochemistry to ruthenocene mechanophores. *Chem. Sci.* **2019**, *10* (19), 4959−4965.
(29) Di Giannantonio, M.; Ayer, M. A.; Verde-Sesto, E.; Lattuada, M.; Weder, C.; Fromm, K. M. Triggered Metal Ion Release and Oxidation: Ferrocene as a Mechanophore in Polymers. *Angew. Chem., Int. Ed.* **2018**, *57* (35), 11445−11450.
(30) Zhang, Y.; Wang, Z.; Kouznetsova, T. B.; Sha, Y.; Xu, E.; Shannahan, L.; Fermen-Coker, M.; Lin, Y.; Tang, C.; Craig, S. L. Distal conformational locks on ferrocene mechanophores guide reaction pathways for increased mechanochemical reactivity. *Nat. Chem.* **2021**, *13* (1), 56−62.
(31) Yan, Y.; Pageni, P.; Kabir, M. P.; Tang, C. Metallocenium chemistry and its emerging impact on synthetic macromolecular chemistry. *Synlett* **2016**, *27* (07), 984−1005.
(32) Zhu, T.; Sha, Y.; Yan, J.; Pageni, P.; Rahman, M. A.; Yan, Y.; Tang, C. Metallo-polyelectrolytes as a class of ionic macromolecules for functional materials. *Nat. Commun.* **2018**, *9* (1), 4329.
(33) Zhu, T.; Zhang, J.; Tang, C. Metallo-Polyelectrolytes: Correlating Macromolecular Architectures with Properties and Applications. *Trends Chem.* **2020**, *2* (3), 227−240.
(34) Haaland, A. Molecular structure and bonding in the 3d metallocenes. *Acc. Chem. Res.* **1979**, *12* (11), 415−422.
(35) Opitz, J. Electron impact ionization of cobalt-tricarbonyl-nitrosyl, cyclopentadienyl-cobalt-dicarbonyl and biscyclopentadienyl-cobalt: appearance energies, bond energies and enthalpies of formation. *Int. J. Mass Spectrom.* **2003**, *225* (2), 115−126.
(36) Rowland, T. G.; Sztaray, B.; Armentrout, P. B. Metal−Cyclopentadienyl Bond Energies in Metallocene Cations Measured Using Threshold Collision-Induced Dissociation Mass Spectrometry. *J. Phys. Chem. A* **2013**, *117* (6), 1299−1309.
(37) Stauf, G. T.; Driscoll, D. C.; Dowben, P. A.; Barfuss, S.; Grade, M. Iron and nickel thin film deposition via metallocene decomposition. *Thin Solid Films* **1987**, *153* (1), 421−430.
(38) Révész, Á.; Szepes, L.; Baer, T.; Sztáray, B. Binding Energies and Isomerization in Metallocene Ions from Threshold Photoelectron Photoion Coincidence Spectroscopy. *J. Am. Chem. Soc.* **2010**, *132* (50), 17795−17803.
(39) Zhang, J.; Yan, Y.; Chance, M. W.; Chen, J.; Hayat, J.; Ma, S.; Tang, C. Charged Metallopolymers as Universal Precursors for Versatile Cobalt Materials. *Angew. Chem., Int. Ed.* **2013**, *52* (50), 13387−13391.
(40) Zhang, J.; Chen, Y. P.; Miller, K. P.; Ganewatta, M. S.; Bam, M.; Yan, Y.; Nagarkatti, M.; Decho, A. W.; Tang, C. Antimicrobial Metallopolymers and Their Bioconjugates with Conventional Antibiotics against Multidrug-Resistant Bacteria. *J. Am. Chem. Soc.* **2014**, *136* (13), 4873−4876.
(41) Yang, P.; Bam, M.; Pageni, P.; Zhu, T.; Chen, Y. P.; Nagarkatti, M.; Decho, A. W.; Tang, C. Trio Act of Boronolectin with Antibiotic-Metal Complexed Macromolecules toward Broad-Spectrum Antimicrobial Efficacy. *ACS Infect. Dis.* **2017**, *3* (11), 845−853.
(42) Cha, Y.; Jarrett-Wilkins, C.; Rahman, M. A.; Zhu, T.; Sha, Y.; Manners, I.; Tang, C. Crystallization-Driven Self-Assembly of Metallo-Polyelectrolyte Block Copolymers with a Polycaprolactone Core-Forming Segment. *ACS Macro Lett.* **2019**, *8* (7), 835−840.
(43) Musgrave, R. A.; Choi, P.; Harniman, R. L.; Richardson, R. M.; Shen, C.; Whittell, G. R.; Crassous, J.; Qiu, H.; Manners, I. Chiral Transmission to Cationic Polycobaltocenes over Multiple Length Scales Using Anionic Surfactants. *J. Am. Chem. Soc.* **2018**, *140* (23), 7222−7231.
(44) Qiu, H.; Gilroy, J. B.; Manners, I. DNA-induced chirality in water-soluble poly(cobaltoceniumethylene). *Chem. Commun.* **2013**, *49* (1), 42−44.

https://doi.org/10.1021/jacs.1c05233
J. Am. Chem. Soc. 2021, 143, 11871−11878

(45) Zhu, T.; Sha, Y.; Firouzjaie, H. A.; Peng, X.; Cha, Y.; Dissanayake, D. M. M. M.; Smith, M. D.; Vannucci, A. K.; Mustain, W. E.; Tang, C. Rational Synthesis of Metallo-Cations Toward Redox- and Alkaline-Stable Metallo-Polyelectrolytes. *J. Am. Chem. Soc.* **2020**, *142* (2), 1083−1089.
(46) Zhu, T.; Xu, S.; Rahman, A.; Dogdibegovic, E.; Yang, P.; Pageni, P.; Kabir, M. P.; Zhou, X.-d.; Tang, C. Cationic Metallo-Polyelectrolytes for Robust Alkaline Anion-Exchange Membranes. *Angew. Chem., Int. Ed.* **2018**, *57* (9), 2388−2392.
(47) Beladi-Mousavi, S. M.; Sadaf, S.; Hennecke, A.-K.; Klein, J.; Mahmood, A. M.; Rüttiger, C.; Gallei, M.; Fu, F.; Fouquet, E.; Ruiz, J.; Astruc, D.; Walder, L. The Metallocene Battery: Ultrafast Electron Transfer Self Exchange Rate Accompanied by a Harmonic Height Breathing. *Angew. Chem., Int. Ed.* **2021**, *60* (24), 13554−13558.
(48) Sha, Y.; Zhu, T.; Rahman, M. A.; Cha, Y.; Hwang, J.; Luo, Z.; Tang, C. Synthesis of site-specific charged metallopolymers via reversible addition-fragmentation chain transfer (RAFT) polymerization. *Polymer* **2020**, *187*, 122095.
(49) Bowser, B. H.; Craig, S. L. Empowering mechanochemistry with multi-mechanophore polymer architectures. *Polym. Chem.* **2018**, *9* (26), 3583−3593.
(50) Riordan, A. R.; Jansma, A.; Fleischman, S.; Green, D. B.; Mulford, D. R. Spectrochemical series of cobalt (III). An experiment for high school through college. *Chem. Educator* **2005**, *10*, 115−119.
(51) Klein, I. M.; Husic, C. C.; Kovács, D. P.; Choquette, N. J.; Robb, M. J. Validation of the CoGEF Method as a Predictive Tool for Polymer Mechanochemistry. *J. Am. Chem. Soc.* **2020**, *142* (38), 16364−16381.
(52) Beyer, M. K. The mechanical strength of a covalent bond calculated by density functional theory. *J. Chem. Phys.* **2000**, *112* (17), 7307−7312.
(53) Bader, R. F. A quantum theory of molecular structure and its applications. *Chem. Rev.* **1991**, *91* (5), 893−928.
(54) Bulat, F. A.; Toro-Labbé, A.; Brinck, T.; Murray, J. S.; Politzer, P. Quantitative analysis of molecular surfaces: areas, volumes, electrostatic potentials and average local ionization energies. *J. Mol. Model.* **2010**, *16* (11), 1679−1691.
(55) Pearson, R. G. Recent advances in the concept of hard and soft acids and bases. *J. Chem. Educ.* **1987**, *64* (7), 561−567.

https://doi.org/10.1021/jacs.1c05233
J. Am. Chem. Soc. 2021, 143, 11871−11878